9. J. T. Ye *et al.*, *Nat. Mater.* **9**, 125 (2010).
10. Y. Lee *et al.*, *Phys. Rev. Lett.* **106**, 136809 (2011).
11. M. M. Qazilbash *et al.*, *Science* **318**, 1750 (2007).
12. M. Liu *et al.*, *Nature* **487**, 345 (2012).
13. F. J. Morin, *Phys. Rev. Lett.* **3**, 34 (1959).
14. M. Nakano *et al.*, *Nature* **487**, 459 (2012).
15. M. Imada, A. Fujimori, Y. Tokura, *Rev. Mod. Phys.* **70**, 1039 (1998).
16. See supplementary materials on *Science* Online.
17. J. Cao *et al.*, *Nat. Nanotechnol.* **4**, 732 (2009).
18. N. F. Mott, *Metal Insulator Transitions* (Taylor & Francis, New York, ed. 2, 1990).
19. R. Restori, D. Schwarzenbach, J. R. Schneider, *Acta Crystallogr. B* **43**, 251 (1987).
20. W. H. Rosevear, W. Paul, *Phys. Rev. B* **7**, 2109 (1973).
21. G. Silversmit, D. Depla, H. Poelman, G. B. Marin, R. De Gryse, *J. Electron Spectrosc. Relat. Phenom.* **135**, 167 (2004).
22. A. Janotti *et al.*, *Phys. Rev. B* **81**, 085212 (2010).
23. R. Kötz, M. Carlen, *Electrochim. Acta* **45**, 2483 (2000).

Acknowledgments: We thank V. Deline, A. Kellock, T. Topuria, and P. Rice for sample characterization, B. Hughes for help with device fabrication, and K. Martens and A. Pushp for useful discussions. Supported by the Graduate School "Material Science in Mainz" [Deutsche Forschungsgemeinschaft (DFG) GSC 266] (T.G.), the Multidisciplinary University Research Initiative program of the Army Research Office (grant W911-NF-09-1-0398) (J.J.), a Feodor Lynen Research Fellowship from the Alexander von Humboldt Foundation (T.D.S.), and a stipend from DFG (GR4000/1-1) (T.G.).

Supplementary Materials

www.sciencemag.org/cgi/content/full/339/6126/1402/DC1
Materials and Methods
Supplementary Text
Figs. S1 to S8
Table S1
References (*24*–*31*)

20 September 2012; accepted 24 January 2013
10.1126/science.1230512

Photonic Spin Hall Effect at Metasurfaces

Xiaobo Yin,[1,2] Ziliang Ye,[1] Junsuk Rho,[1] Yuan Wang,[1] Xiang Zhang[1,2]*

The spin Hall effect (SHE) of light is very weak because of the extremely small photon momentum and spin-orbit interaction. Here, we report a strong photonic SHE resulting in a measured large splitting of polarized light at metasurfaces. The rapidly varying phase discontinuities along a metasurface, breaking the axial symmetry of the system, enable the direct observation of large transverse motion of circularly polarized light, even at normal incidence. The strong spin-orbit interaction deviates the polarized light from the trajectory prescribed by the ordinary Fermat principle. Such a strong and broadband photonic SHE may provide a route for exploiting the spin and orbit angular momentum of light for information processing and communication.

The relativistic spin-orbit coupling of electrons results in intrinsic spin precessions and, therefore, spin polarization–dependent transverse currents, leading to the observation of the spin Hall effect (SHE) and the emerging field of spintronics (*1*–*3*). The coupling between an electron's spin degree of freedom and its orbital motion is similar to the coupling of the transverse electric and magnetic components of a propagating electromagnetic field (*4*). To conserve total angular momentum, an inhomogeneity of material's index of refraction can cause momentum transfer between the orbital and the spin angular momentum of light along its propagation trajectory, resulting in transverse splitting in polarizations. Such a photonic spin Hall effect (PSHE) was recently proposed theoretically to describe the spin-orbit interaction, the geometric phase, and the precession of polarization in weakly inhomogeneous media, as well as the interfaces between homogenous media (*5*, *6*).

However, the experimental observation of the SHE of light is challenging, because the amount of momentum that a photon carries and the spin-orbit interaction between the photon and its medium are exceedingly small. The exploration of such a weak process relies on the accumulation of the effect through many multiple reflections (*7*) or ultrasensitive quantum weak measurements with pre- and postselections of spin states (*8*, *9*). Moreover, the present theory of PSHE assumes the conservation of total angular momentum over the entire beam (*5*–*9*), which may not hold, especially when tailored wavelength-scale photonic structures are introduced. In this work, we demonstrate experimentally the strong interactions between the spin and the orbital angular momentum of light in a thin metasurface—a two-dimensional (2D) electromagnetic nanostructure with designed in-plane phase retardation at the wavelength scale. In such an optically thin material, the resonance-induced anomalous "skew scattering" of light destroys the axial symmetry of the system that enables us to observe a giant PSHE, even at the normal incidence. In contrast, for interfaces between two homogeneous media, the spin-orbit coupling does not exist at normal incidence (*5*–*9*).

Metamaterial made of subwavelength composites has electromagnetic responses that largely originate from the designed structures rather than the constituent materials, leading to extraordinary properties including negative index of refraction (*10*, *11*), superlens (*12*), and optical invisibilities (*13*, *14*). As 2D metamaterials, metasurfaces have shown intriguing abilities in manifesting electromagnetic waves (*15*, *16*). Recently, anomalous reflection and refraction at a metasurface has been reported (*17*, *18*), and a variety of applications, such as flat lenses, have been explored (*19*–*22*). However, the general approach toward metasurfaces neglects the spin degree of freedom of light, which can be substantial in these materials. We show here that the rapidly varying in-plane phase retardation that is dependent on position along the metasurface introduces strong spin-orbit interactions, departing the light trajectory (S) from what is depicted by Fermat principles, $S = S_{Fermat} + S_{SO}$ (where S_{SO}

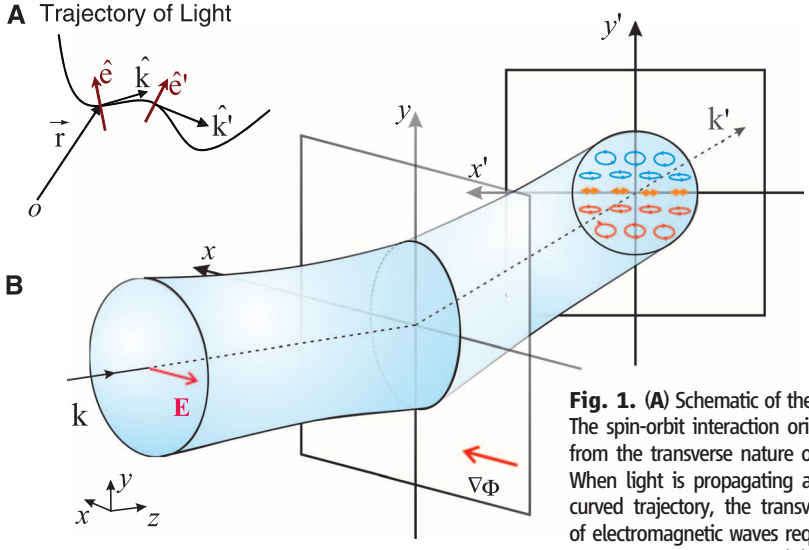

Fig. 1. **(A)** Schematic of the PSHE. The spin-orbit interaction originates from the transverse nature of light. When light is propagating along a curved trajectory, the transversality of electromagnetic waves requires a rotation in polarization. **(B)** Transverse polarization splitting induced by a metasurface with a strong gradient of phase retardation along the x direction. The rapid phase retardation refracts light in a skewing direction and results in the PSHE. The strong spin-orbit interaction within the optically thin material leads to the accumulation of circular components of the beam in the transverse directions (y' directions) of the beam, even when the incident angle is normal to the surface.

[1]National Science Foundation Nanoscale Science and Engineering Center, 3112 Etcheverry Hall, University of California at Berkeley, Berkeley, CA 94720, USA. [2]Materials Sciences Division, Lawrence Berkeley National Laboratory (LBNL), 1 Cyclotron Road, Berkeley, CA 94720, USA.

*Corresponding author. E-mail: xiang@berkeley.edu

is a correction to the light trajectory raised from the metasurface-induced spin-orbit interaction).

The PSHE or the spin-orbit interaction arises from the noncolinear momentum and velocity (the change of trajectory) of light. When light is propagating along a curved trajectory (Fig. 1A), the time-varying momentum along the light path must introduce a geometric polarization rotation to maintain the polarization transverse to its new propagation direction (*23*), $\dot{\hat{e}} = -\mathbf{k}(\hat{\mathbf{e}} \cdot \dot{\mathbf{k}})/k^2$. Here, $\hat{\mathbf{e}}$ and $\mathbf{k}$ are the polarization vector and the wave vector, respectively, $\dot{\mathbf{k}}$ is the change of the propagation direction, and k is the amplitude of the wave vector. The rotation of the polarization depends on the helicity of light and may be considered as circular birefringence with a pure geometric origin (*23*–*25*). As the back-action from geometric polarization rotations, the spin-orbit interaction also changes the propagation path of light, as we will show in later sections, resulting in a helicity-dependent transverse displacement for light; i.e., photonic SHE.

For an ordinary interface between two homogeneous media, when a Gaussian beam impinges onto the interface at normal incidence, the axial symmetry normal to the surface eliminates the spin-orbit coupling, and the total angular momentum of the entire beam is conserved. However, by designing a metasurface with a rapid gradient of phase discontinuity $\nabla\Phi$ along the interface in the x direction (Fig. 1B), we introduce a strong spin-orbit coupling when the light is refracted off the interface. The rapid, wavelength-scale phase retardation can be incorporated in the optical path by suitable design of the interface (*17*, *18*, *26*). Such a position-dependent phase discontinuity removes the axial symmetry of the interface and, therefore, allows us to observe the PSHE, even at the normal incident angle. Figure 1B schematically depicts the PSHE for the light beam that is refracted off a metasurface with rapid in-plane phase retardation. The momentum conservation at the metasurface now must take into account that the position-dependent phase retardation and the induced effective circular birefringence are determined by the gradient of the in-plane phase change or the curvature of the ray trajectory, $(\dot{\mathbf{k}} \times \mathbf{k})/k^2$ (*7*), where $\dot{\mathbf{k}}$ depends on the rapid phase change. For a linearly polarized incidence, light of opposite helicities will be accumulated at the opposite edges of an anomalously refracted beam in the transverse direction (Fig. 1B). The faster the in-plane phase changes, the stronger the effect becomes. Because both the local phase response and its gradient are tailored through metamaterial design, the optical spin-orbit interaction from the metasurface is strong, broadband, and widely tunable.

To experimentally observe the strong PSHE at the metasurfaces, we used a polarization-resolved detection setup (Fig. 2), which allows precise measurement of Stokes parameters of the refracted beam, providing the spin-state information of the light in the far field. A supercontinuum light source is used for broadband measurement, and

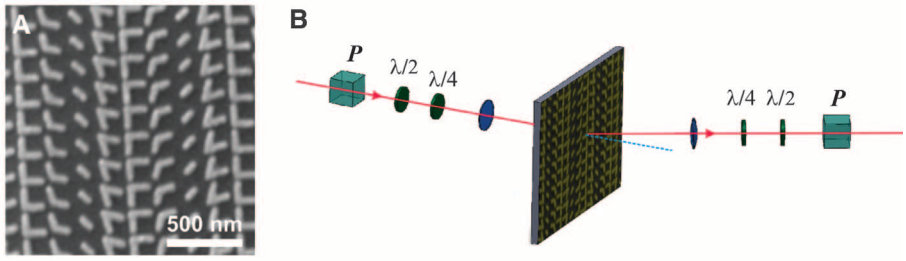

Fig. 2. (**A**) Scanning electron microscope image of a metasurface with a rapid phase gradient in the horizontal (x) direction. The period of the constituent V-shaped antenna is 180 nm. Eight antennas with different lengths, orientations, and spanning angles were chosen for a linear phase retardation, ranging from 0 to 2π with π/4 intervals. Scale bar, 500 nm. (**B**) Light from a broadband source was focused onto the sample with a lens (focal length f = 50 mm). The polarization can be adjusted in both the x and y directions with a half-wave plate. The regularly and anomalously refracted far-field transmission through the metasurface was collected using a lens (f = 50 mm) and imaged on an InGaAs camera. The polarization state of the transmission is resolved by using an achromatic quarter-wave plate (λ/4), a half-wave plate (λ/2), and a polarizer with a high extinction ratio. *P*, polarizer.

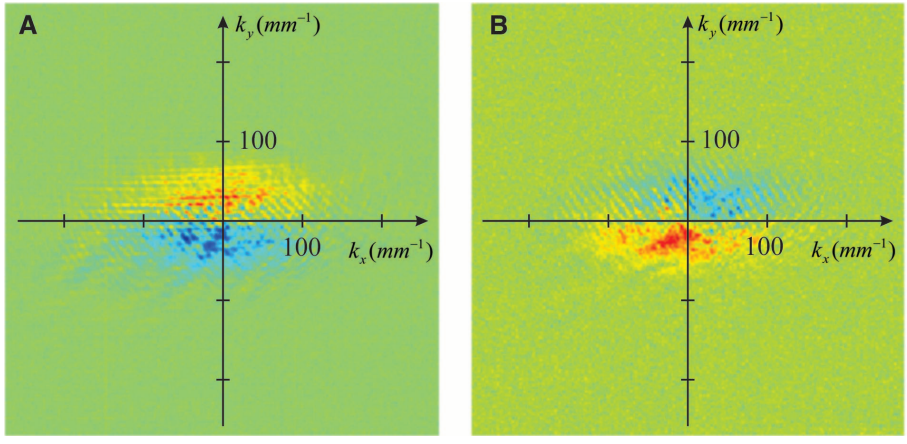

Fig. 3. (**A**) Observation of a giant SHE: the helicity of the anomalously refracted beam. The incidence is from the silicon side onto the metasurface and is polarized along the x direction along the phase gradient. The incidence angle is at surface normal. Red and blue represent the right and left circular polarizations, respectively. (**B**) Helicity of the refracted beam with incidence polarized along the y direction.

the beam is focused onto the sample with a spot size of ~50 μm. Our metasurfaces consist of V-shaped gold antennas. By changing the length and orientation of the arms of the V-shaped structures, the subwavelength antennas at resonance introduce tunable phase retardations between the incident and the forward-propagating fields. For linear phase retardation along the x direction, we chose eight antennas with optimized geometry parameters. We measured samples with different phase gradients; a scanning electron microscope image of the antenna array with a phase gradient of 4.4 rad/μm is shown in Fig. 2A as one example. We used a lens of 50-mm focal length to collect the anomalously refracted far-field transmission through the metasurface, and we imaged this transmission on an InGaAs camera. The polarization of the incidence is linear and can be adjusted in either the x or y directions with a half-wave plate. The polarization states of the anomalously and the regularly refracted beams are resolved at the far field using an achromatic quarter-wave plate, a half-wave plate, and a polarizer with an extinction ratio greater than 10^5 for all wavelengths of interest.

Because the polarization state of light is unambiguously determined by the Stokes vector $\vec{\mathbf{S}}$ on a unit Poincaré sphere, the evolution of the polarization due to spin-orbit interaction is well described by the precession of the Stokes vector on a Poincaré sphere. The helicity or the handedness of light is given by the circular Stokes S_z parameter (circular polarization) $S_z = \frac{I_{\sigma^+} - I_{\sigma^-}}{I_{\sigma^+} + I_{\sigma^-}}$, where I_{σ^+} and I_{σ^-} are the intensities of the anomalous refraction with circular polarization basis, which were imaged successively using the camera. The coordinates of the image represent the in-plane wave vectors of the refracted beams. The right circular σ^+ and left circular σ^- polarizations are discriminated by setting appropriately the angle of the wave plates and polarization analyzer. Using the polarization-resolved detection, we calculated the circular Stokes parameter of the anomalously refracted beam from measurements for each pixel; this is shown in Fig. 3A for x-polarized incidence. The in-plane wave vector dependence

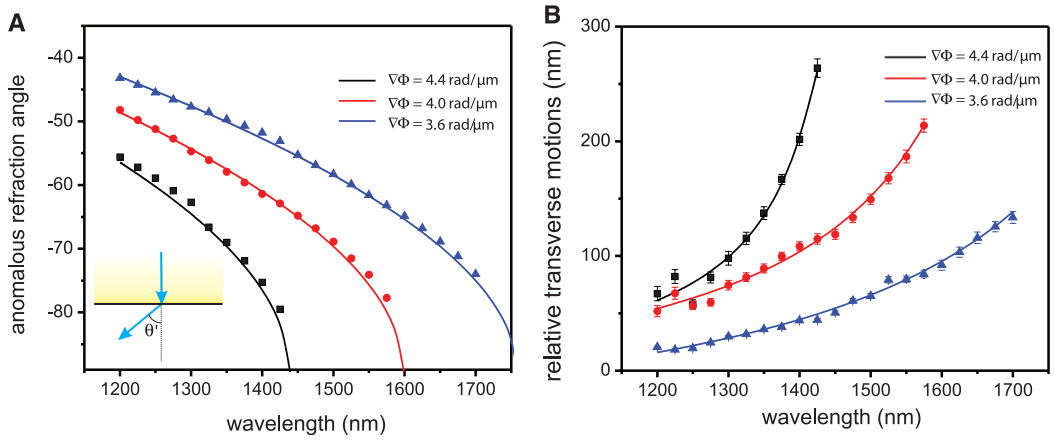

Fig. 4. (**A**) Wavelength dependence of the refraction angles when excitation is normally incident onto the metasurface. The measurement was conducted for three samples with different phase gradients of 3.6, 4.0, and 4.4 rad/μm. The measured refraction angles agree well with the theoretical predictions (solid curves). The angles are the same for both the left and right circularly polarized light. (Inset) Schematic depiction of the light trajectory for the anomalous refraction for the surface normal incidence. (**B**) Transverse motion (data points with error bars) between anomalously refracted light beams with right and left circular polarizations, showing a PSHE effect over a broad range of wavelengths. Solid curves are a guide for the eyes. The measurement was performed for three metasurfaces with different phase gradients. The incidence was kept at surface normal but was periodically modulated between the left and right circular polarizations. Any transverse motion of the weight center of the beam was detected by a position-sensitive detector.

of the circular Stokes parameters shows a maximal value of ~0.1 located at $\pm\pi/2$, and the sign of S_z is reversed between $+\pi/2$ and $-\pi/2$, showing a transverse motion of the polarization. Whereas the incident angle is kept at zero throughout the experiment, the phase gradient along the interface removes the axial symmetry of the optical system and enables the direct observation of the PSHE for the anomalously refracted beams with different circularly polarized light. Figure 3B shows the PSHE effect for *y*-polarized incidence: The helicity of the refracted beam is clearly inverted due to the 90° phase rotation of the incidence. As the transverse spin current is solely determined by the longitudinal components of electromagnetic fields, such a distinct PSHE can only be observed in the anomalously refracted beam. As a control experiment, the spin-orbit coupling vanishes for the regularly transmitted beam, which exits the metasurface in the direction of the surface normal.

The photonic spin-orbit interaction in a curved light path not only manifests a helicity-dependent circular birefringence but also influences the trajectory of light. This effect resembles the Imbert-Fedorov shifts in the case of total internal reflections (*27*) and the recently observed optical Magnus effect at the near field (*28*, *29*). When considering spin-orbit coupling, the ordinary Fermat principle based on ray optics is not sufficient in predicting the light trajectory; therefore, a helicity-dependent transverse motion of light emerges from the additional geometric phases due to spin-orbit interaction. For the incident light with a pure spin state (circularly polarized), a transverse motion of the beam's center of mass is thus expected.

Such a transverse motion occurs in real space and can be directly measured. Replacing the polarization optics shown in Fig. 2B with a variable liquid-crystal phase retarder, we measured the spin-dependent motion of photons (the relative displacement between the anomalously refracted I_{σ^+} and I_{σ^-}) by an InGaAs quadrant detector with polarized incident beam periodically modulated in either left- (σ^+) or right-handed (σ^-) polarization states. Throughout the experiment, the incidence angle was kept at normal incidence to the sample. The tailored in-plane phase gradient induces anomalous transmission at different refracting angles determined by the gradient. Figure 4A shows the refraction angle at different incident wavelengths for multiple samples with different phase gradients. The anomalous refraction angle approaches 90° when the incident wavelength approaches eight times the period of the V-shaped antennas. In Fig. 4B, the transverse motions of the beams are shown at the normal incident for wavelengths over hundreds of nanometers in bandwidth. The feedback from the polarization clearly deviates the trajectory from that given by the ordinary Fermat Principle. The strong spin-orbit interactions induced by the resonant V-shaped antenna array enable the observation of the transverse displacement, which increases rapidly as the anomalous refraction angle approaches 90°. Current PSHE theory assumes the conserved momentum solely over the Gaussian wave packet. However, the rapid phase gradient along the metasurface supplies additional momentum, making such a theoretical treatment incomplete. A new apparatus for analytical analysis should be developed to account for such a rapid phase gradient along the surface. By considering the energy transport at the interface, however, the polarization-dependent transverse motion of light can be analyzed by integrating the Poynting vectors (including the evanescent fields) over the half-space of the exiting medium (see the supplementary materials).

The strong photonic SHE at a metasurface with a designed phase discontinuity over the wavelength scale enables the observation of transverse motions of circularly polarized light. The anomalous skew scattering of light simultaneously breaks the rotational symmetry in the polarization space and the axial symmetry along its trajectory, giving rise to a broadband PSHE, even at the normal incidence. The generation and manipulation of strong spin-orbit interaction of light with tailored nanomaterials provide a new degree of freedom in information transfer between spin and orbital angular momentum of photons.

References and Notes

1. E. Hirsch, *Phys. Rev. Lett.* **83**, 1834 (1999).
2. S. A. Wolf *et al.*, *Science* **294**, 1488 (2001).
3. T. Jungwirth, J. Wunderlich, K. Olejník, *Nat. Mater.* **11**, 382 (2012).
4. B. A. Bernevig, X. W. Yu, S. C. Zhang, *Phys. Rev. Lett.* **95**, 076602 (2005).
5. M. Onoda, S. Murakami, N. Nagaosa, *Phys. Rev. Lett.* **93**, 083901 (2004).
6. K. Y. Bliokh, Y. P. Bliokh, *Phys. Rev. Lett.* **96**, 073903 (2006).
7. K. Bliokh, A. Niv, V. Kleiner, E. Hasman, *Nat. Photonics* **2**, 748 (2008).
8. O. Hosten, P. Kwiat, *Science* **319**, 787 (2008).
9. Y. Gorodetski *et al.*, *Phys. Rev. Lett.* **109**, 013901 (2012).
10. J. B. Pendry, *Phys. Rev. Lett.* **85**, 3966 (2000).
11. R. A. Shelby, D. R. Smith, S. Schultz, *Science* **292**, 77 (2001).
12. N. Fang, H. Lee, C. Sun, X. Zhang, *Science* **308**, 534 (2005).
13. J. B. Pendry, D. Schurig, D. R. Smith, *Science* **312**, 1780 (2006).
14. J. Valentine, J. Li, T. Zentgraf, G. Bartal, X. Zhang, *Nat. Mater.* **8**, 568 (2009).
15. F. Falcone *et al.*, *Phys. Rev. Lett.* **93**, 197401 (2004).
16. S. L. Sun *et al.*, *Nat. Mater.* **11**, 426 (2012).
17. N. Yu *et al.*, *Science* **334**, 333 (2011).
18. X. Ni, N. K. Emani, A. V. Kildishev, A. Boltasseva, V. M. Shalaev, *Science* **335**, 427 (2012).
19. Y. Zhao, A. Alù, *Phys. Rev. B* **84**, 205428 (2011).
20. P. Genevet *et al.*, *Appl. Phys. Lett.* **100**, 013101 (2012).
21. F. Aieta *et al.*, *Nano Lett.* **12**, 4932 (2012).
22. M. A. Kats *et al.*, *Proc. Natl. Acad. Sci. U.S.A.* **109**, 12364 (2012).
23. V. S. Liberman, B. Y. Zel'dovich, *Phys. Rev. E* **49**, 2389 (1994).
24. R. Y. Chiao, Y. S. Wu, *Phys. Rev. Lett.* **57**, 933 (1986).
25. M. V. Berry, *Nature* **326**, 277 (1987).
26. D. R. Smith, J. J. Mock, A. F. Starr, D. Schurig, *Phys. Rev. E* **71**, 036609 (2005).
27. O. Costa de Beauregard, C. Imbert, Y. Levy, *Phys. Rev. D* **15**, 3553 (1977).
28. K. Y. Bliokh, Y. Gorodetski, V. Kleiner, E. Hasman, *Phys. Rev. Lett.* **101**, 030404 (2008).
29. Y. Gorodetski, A. Niv, V. Kleiner, E. Hasman, *Phys. Rev. Lett.* **101**, 043903 (2008).

Acknowledgments: This research is supported by the U.S. Department of Energy, Office of Basic Energy Sciences under contract no. DE-AC02-05CH11231 through the Materials Sciences Division of LBNL. J.R. acknowledges a fellowship from the Samsung Scholarship Foundation, Republic of Korea. We thank S. Dhuey and S. Cabrini of the Molecular Foundry at LBNL for their help on electron beam lithography over large areas.

Supplementary Materials

www.sciencemag.org/cgi/content/full/339/6126/1405/DC1
Supplementary Text
Fig. S1
References (*30*, *31*)

19 October 2012; accepted 9 January 2013
10.1126/science.1231758

Photonic Spin Hall Effect at Metasurfaces

Xiaobo Yin *et al.*

Science **339**, 1405 (2013);
DOI: 10.1126/science.1231758